Letter

Solid-state ^{229}Th nuclear laser with two-photon pumping

Haowei Xu,[1] Hao Tang,[2] Guoqing Wang,[1,3] Changhao Li,[1,3] Boning Li,[3,4] Paola Cappellaro,[1,3,4,*] and Ju Li[1,2,†]

[1]*Department of Nuclear Science and Engineering, Massachusetts Institute of Technology, Cambridge, Massachusetts 02139, USA*
[2]*Department of Materials Science and Engineering, Massachusetts Institute of Technology, Cambridge, Massachusetts 02139, USA*
[3]*Research Laboratory of Electronics, Massachusetts Institute of Technology, Cambridge, Massachusetts 02139, USA*
[4]*Department of Physics, Massachusetts Institute of Technology, Cambridge, Massachusetts 02139, USA*

(Received 8 May 2023; accepted 25 July 2023; published 24 August 2023)

The radiative excitation of the 8.3 eV isomeric state of ^{229}Th is an long-standing challenge due to the lack of tunable far-ultraviolet (FUV) sources. In this work, we propose an efficient two-photon pumping scheme for ^{229}Th using the optonuclear quadrupolar effect, which only requires a 300 nm UV-B pumping laser. We further demonstrate that population inversion between the nuclear isomeric and ground states can be achieved at room temperature using a two-step pumping process. The nuclear laser, which has been pursued unsuccessfully for decades, may be realized using a watt-level UV-B pumping laser and ultrawide band gap thorium compounds (e.g., ThF_4, Na_2ThF_6, or K_2ThF_6) as the gain medium.

DOI: 10.1103/PhysRevA.108.L021502

I. INTRODUCTION

The ^{229}Th nucleus exhibits a long-lived isomeric state (^{229*}Th) with an ultralow energy of $\omega_{is} \approx 8.3$ eV above the ground state [1–3], in stark contrast to the typical nuclear excitation energies (keV to MeV) [4]. Such a low-energy isomeric state elicits considerable interest in understanding the underlying nuclear structure [5,6] and the coupling between nuclear and electronic excitations [7–9], as well as in developing various applications such as creating a nuclear clock frequency standard [1,10–12] and determining fundamental physical constants [13,14].

^{229}Th also provides unique opportunities for building nuclear lasers, which were envisioned more than half a century ago, but have not been realized yet [15–17]. Besides the conceptual importance of nuclear lasing, nuclear lasers also feature short wavelengths and narrow linewidths that could facilitate various applications. ^{229}Th nuclear lasers, if realized, could also offer a direct and convenient approach to optically pump ^{229}Th nuclei, which is crucial for many applications involving ^{229}Th, including the nuclear clock [1,10–12]. However, the construction of nuclear lasers is a demanding task that requires interdisciplinary research in nuclear physics, materials science, and photonics. A major challenge is that lasers typically require population inversion and hence efficient pumping to the excited states. However, it is notoriously difficult to pump the nuclear excited states. Historically, it has been proposed to use x-ray radiations, slow neutron capture, or other nuclear reactions to pump the nuclear excited states, all of which are not so efficient [15]. For ^{229}Th, it is possible to populate the isomeric states optically, thanks to the small transition energy within the far-ultraviolet (FUV) regime [17]. Unfortunately, FUV sources resonant with the ^{229}Th isomeric transition are still under development, and the direct laser excitation of ^{229}Th has not been experimentally demonstrated yet [1]. Moreover, even if direct FUV pumping becomes available, population inversion still cannot be achieved if only two states are involved, and at least one auxiliary state is necessary. For nuclear lasers, it is not straightforward to find the auxiliary state [17], because the energy gaps between nuclear spin sublevels (10^{-9}–10^{-6} eV) are too small compared with typical laser frequency ($\sim$1 eV), thus requiring prohibitively low temperatures [17]. Meanwhile, the energy gaps between nuclear orbital excited states are too large—the second excited state of ^{229}Th is around 29 keV above the ground state—thus requiring demanding x-ray sources.

In this work, we propose a nuclear laser based on ^{229}Th with a two-step two-photon pumping, which could potentially overcome the aforementioned challenges. As the gain medium, we suggest using thorium compounds such as Na_2ThF_6, which can provide a high number density of ^{229}Th and an ultrawide band gap, $E_g > \omega_{is}$ [18]. The ultrawide band gap also forbids internal conversion (IC) of the isomeric state [1,4], because the large ionization energy prevents this nonradiative nuclear decay process that excites and ejects a valence electron [19]. These properties are advantageous for the nuclear laser. Then, we introduce the two-photon pumping of the ^{229}Th isomeric states based on the optonuclear quadrupolar (ONQ) effect [20,21], which is an efficient interface between two photons and the nuclei. The ONQ pumping requires only a near-ultraviolet laser operating at $\omega_{in} = \frac{\omega_{is}}{2} \approx 4.2$ eV, which is in the UV-B regime and could be much easier to build than a FUV laser [22]. In contrast to the pumping scheme based on the electronic bridge (EB) effect [7,9,23–26], the ONQ pumping avoids the usage of lasers resonant with electronic transitions and can thus significantly suppress the heating in the solid-state gain medium. This is important when the ^{229}Th density is high and the pumping laser is strong, whereby the

*pcappell@mit.edu
†liju@mit.edu

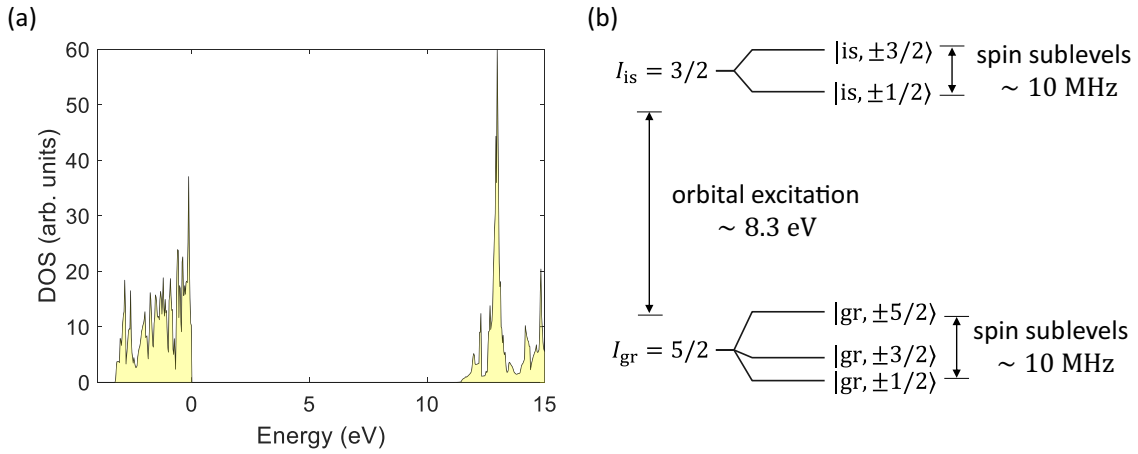

FIG. 1. (a) Electronic density of states of Na_2ThF_6 from G_0W_0 calculations. (b) Nuclear energy level diagram of ^{229}Th in Na_2ThF_6.

heating power density will be high. Under a sub-watt-level pumping laser, the ONQ pumping could be fast enough for the experimental observation of the radiative excitations of ^{229*}Th, which has not been realized yet. We further propose a two-step pumping process to achieve population inversion at room temperature, taking advantage of the long relaxation time of ^{229}Th nuclear states. We show that the peak power of the nuclear laser can reach watt level when the gain medium size is about 1 μm × 1 μm × 1 mm. By selecting different nuclear spin sublevels, the nuclear laser can have tunable chirality as well [27]. The nuclear laser can have a narrow linewidth, and can naturally match the resonance condition for optically pumping the ^{229}Th nuclear clock. While ^{229}Th can be pumped with other schemes under development or operation [2], the nuclear laser pumping may have its own advantage. For example, the central frequency of the nuclear laser can potentially be tuned with ultrafine resolution using, e.g., the Mössbauer effect. Further investigation is required to explore the potential applications of the nuclear laser.

II. ^{229}Th IN ULTRAWIDE BAND GAP Th COMPOUNDS

The radiative transitions between the isomeric (angular momentum $I_{is} = 3/2$) and ground states ($I_{gr} = 5/2$) of ^{229}Th have both $M1$ (magnetic dipole) and $E2$ (electric quadrupole) channels. Some detailed information on the isomeric transition, including the selection rules, is summarized in Sec. 2 in the Supplemental Material [28] (see also Refs. [5,6,29–38] cited therein). The spontaneous gamma decay of ^{229*}Th is dominated by the $M1$ process with a decay rate of $\gamma_{is}^{\gamma} \sim 10^{-4}$ Hz [4]. The IC, while fast [39], can be forbidden if the isomeric transition energy ω_{is} is below the electron ionization energy, so that the nuclear transition does not have enough energy to kick out an electron. In this case, the total decay rate of ^{229*}Th is $\gamma_{is}^{decay} = \gamma_{is}^{\gamma}$ [40]. It has been shown that using trapped ionized ^{229}Th [41] or ^{229}Th dopants in ultrawide band gap compounds (e.g., CaF_2 [42]) can forbid IC. For nuclear lasers, it is desirable to have a large number density of ^{229}Th. Hence, we instead suggest using natural Th compounds with ultrawide electronic band gaps, which can have a number density of up to 10^{26} m^{-3} if ^{229}Th is enriched to 1% isotopic abundance. Some candidate compounds are ThF_4, Na_2ThF_6, and K_2ThF_6, all of which have electronic band gaps $E_g \gtrsim 10$ eV according to experiments [18] as well as our many-body G_0W_0 calculations (Sec. 1.1 in Ref. [28]).

We will use Na_2ThF_6 as an example. According to our calculations, the electronic band gap of Na_2ThF_6 is $E_g \approx 11$ eV [Fig. 1(a)], yielding $\omega_{is} < E_g < \frac{3}{2}\omega_{is}$. The splitting between nuclear spin sublevels due to the nuclear quadrupolar interaction is on the order of 10 MHz [40 neV, Fig. 1(b)], equivalent to a temperature of mK. Hence, under ambient conditions, the five ground-state sublevels are almost equally populated. In contrast, ω_{is} is much greater than the thermal energy, and the isomeric sublevels should have zero population at thermal equilibrium. Another important parameter for the nuclear laser is the drift (inhomogeneous broadening) γ_{is}^{drift} of the isomeric transition energy in solid-state compounds, which could result from magnetic interactions, temperature, and strain effects [31]. The magnetic dipole interaction between nearby nuclei is on the order of kHz [43], while our calculations (Sec. 1.1 in Ref. [28]) indicate that γ_{is}^{drift} can be kept below 10 kHz if the variance of strain (temperature) is below 10^{-2} % (1 K). Hence, we will assume $\gamma_{is}^{drift} \sim 10$ kHz in the following. The small drift in the isomeric transition energy also indicates that the nuclear laser can have a narrow linewidth.

III. TWO-PHOTON PUMPING VIA THE OPTONUCLEAR QUADRUPOLAR EFFECT

As discussed before, the pumping of the nuclear isomeric excited state is a key challenge for nuclear lasers. In this section, we demonstrate the two-photon pumping of ^{229}Th based on the ONQ effect [20,21]. Specifically, the nuclear state can be influenced by the nuclear quadrupolar ($E2$) interaction $\mathcal{H}_{E2} = \mathcal{M}_{E2}\mathcal{V}$, which is an electromagnetic interaction between the nuclear electric quadrupolar moment $\mathcal{M}_{E2}$ and the electric field gradient (EFG) $\mathcal{V}$ at the site of the nucleus. External fields can modulate $\mathcal{V}$, which can in turn control the nuclear states. In fact, the gamma decay through the $E2$ channel is the consequence of the oscillating EFG of a resonant photon [44]. However, the EFG of a FUV photon is too weak, and thus the $E2$ channel for gamma decay is inefficient compared with the $M1$ channel for bare ^{229*}Th in vacuum [6].

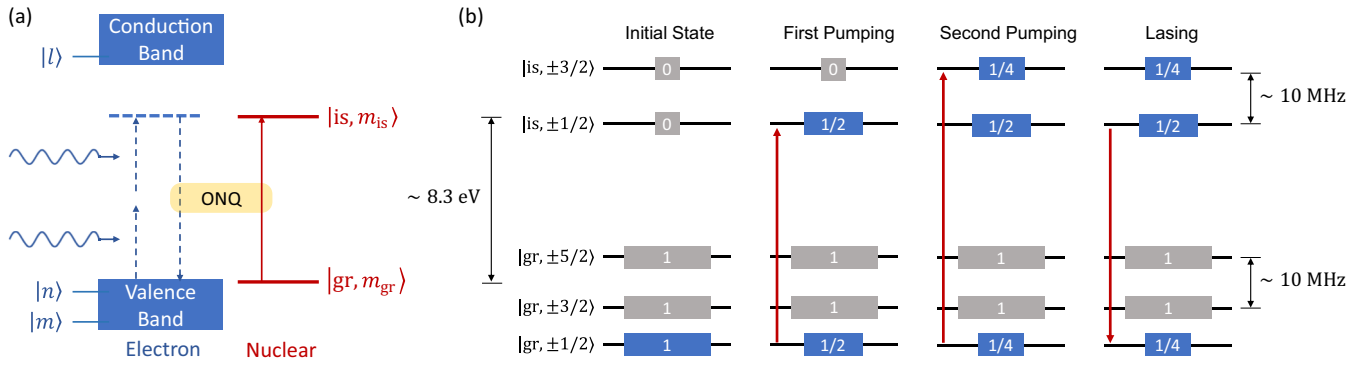

FIG. 2. (a) Two-photon pumping scheme based on the ONQ effect. Two photons pump a (virtual) electronic excitation, which is then swapped to a real nuclear excitation through the nuclear quadrupolar interaction. (b) The two-step pumping scheme to achieve population inversion. Numbers in the boxes indicate normalized populations. States with gray boxes do not participate in the nuclear pumping/lasing process.

The situation is different when electrons come into play. The electric field generated by electrons can vary by $\Delta\mathcal{E}_e \gtrsim 1$ V/Å over the atomic scale a_0, with a_0 the Bohr radius. Hence, the EFG $\mathcal{V}_e$ generated by electrons can reach $\mathcal{V}_e \sim \frac{\Delta\mathcal{E}_e}{a_0} \sim 1$ V/Å^2, leading to a strong nuclear quadrupolar interaction (MHz to GHz). When the electronic states are perturbed, the change in the nuclear quadrupolar interaction is proportionally strong. This fact helps explain the fast IC of ^{229*}Th through the $E2$ channel [19].

Particularly, the electronic states can be perturbed by two-photon transitions. This is the origin of various well-known second-order nonlinear optical effects—two photons drive the electronic orbital motions, which in turn generate, e.g., electromagnetic waves (sum or difference frequency generation) or phonons (Raman scattering). Similarly, electronic orbital motions can also generate oscillating EFG and hence oscillating nuclear quadrupolar interaction, which can influence the nuclear states. This is the ONQ effect [20,21], which can be described by the Hamiltonian $\mathcal{H}_{E2}^{\mathrm{ONQ}}(t) = \sum_{ij} \mathcal{D}_{ij,\pm}^{pq} \mathcal{E}_p \mathcal{E}_q e^{i(\omega_p \pm \omega_q)t} + \mathrm{H.c.}$, where $\mathcal{E}_{p,q}$ and $\omega_{p,q}$ are the electric field strength and the frequency of the two photons p and q, respectively. The $\pm$ sign indicates the sum (+) or difference (−) frequency process. The response function $\mathcal{D}_{ij,\pm}^{pq} = \mathcal{M}_{E2} \frac{\partial^2 \mathcal{V}_{ij}}{\partial \mathcal{E}_p \partial \mathcal{E}_q}$ can be expressed as [20,21]

$$\mathcal{D}_{ij,\pm}^{pq} = \mathcal{M}_{E2} \sum_{mnl} \frac{[\mathcal{V}_{ij}]_{mn}}{\omega_{mn} - (\omega_p \pm \omega_q)} \left\{ \frac{f_{lm}[r_p]_{nl}[r_q]_{lm}}{\omega_{ml} - \omega_p} - \frac{f_{nl}[r_q]_{nl}[r_p]_{lm}}{\omega_{ln} - \omega_p} \right\} + (p \leftrightarrow q), \tag{1}$$

where $(p \leftrightarrow q)$ indicates the exchange of the p and q subscripts. $[r_i]_{nl} \equiv \langle n|r_i|l\rangle$ and $[\mathcal{V}_{ij}]_{mn} = \frac{e}{4\pi\varepsilon_0}\langle m|\frac{3r_i r_j - \delta_{ij} r^2}{r^5}|n\rangle$ are the electron position and EFG operators, respectively, where m, n, l label the electronic states, and ε_0 is the vacuum permittivity. ω_{mn} (f_{mn}) is the energy (occupation) differences between two electronic states $|m\rangle$ and $|n\rangle$ (Planck constant $\hbar = 1$). Here, we focus on the sum-frequency term $e^{i(\omega_p+\omega_q)t}$, which can pump the electrons to a (virtual) excited state with an energy of $\omega_p + \omega_q$. Then, the nuclear excitation can be realized by a swap process between the electronic and nuclear excitations—electrons (virtually) jump back to the ground state, while the nucleus jumps to the isomeric state [Fig. 2(a)]. This process is enabled by the electron-nuclear interactions, which can have $M1$, $E2$, and other higher-order channels. In the case of Na_2ThF_4, there are no net electron spins, so the $M1$ channel is absent. To leading order, we only need to consider the $E2$ channel.

When $\omega_p + \omega_q < E_g$, the electronic transition is virtual, but the nuclear transition can be a real resonant transition when $\omega_p + \omega_q = \omega_{\mathrm{is}}$. When the laser frequencies (ω_p, ω_q or $\omega_p + \omega_q$) are resonant with an electronic transition, the electrons can be resonantly pumped to electronic excited states, and the $\mathcal{D}$ tensor will be substantially enhanced. In this case, the ONQ effect is in principle equivalent to the EB process [7,9,23–26]. We would like to emphasize that a unique advantage of the ONQ effect is that the laser frequencies can be off resonant with electronic transitions (below band gap), which can significantly suppress the one-photon absorption of laser energy and the resultant heating. This difference with the EB process is particularly important when the number density of Th is high and the pumping laser is strong, both of which are desirable for the solid-state nuclear laser. Additionally, the EB process is not favorable in an ultrawide band gap thorium compound, whereby the one-photon resonant transition requires a laser with frequency >10 eV, which is hard to construct. Therefore, we believe the ONQ effect can be more advantageous than the EB process regarding building the solid-state nuclear laser.

For an order of magnitude estimation, we only consider the (m, n, l) pair that has ω_{mn}, ω_{ml} close to E_g, which makes a major contribution to $\mathcal{D}$. We also use $\langle m|\frac{3r_i r_j - \delta_{ij} r^2}{r^5}|n\rangle \approx \frac{1}{a_0^3}$ and $[r_i]_{mn} \approx a_0$, as the spatial distribution of the electronic states is characterized by a_0. We also set $\omega_p = \omega_q = \omega_{\mathrm{in}} = \frac{\omega_{\mathrm{is}}}{2}$. Finally, one has $\mathcal{D}_+ \sim \mathcal{M}_{E2} \frac{g_S e^3}{4\pi\varepsilon_0 a_0} \frac{1}{(E_g - \omega_{\mathrm{is}})(E_g - \omega_{\mathrm{is}}/2)}$, where $g_S = 2$ is the electron spin degeneracy.

The pumping rate to the isomeric state is $R = \frac{4|\langle \mathrm{gr}, m_{\mathrm{gr}}|\mathcal{D}_+|\ \mathrm{is}, m_{\mathrm{is}}\rangle|^2 \mathcal{E}^4}{\Gamma_{\mathrm{pump}}}$ with $\Gamma_{\mathrm{pump}} \sim \gamma_{\mathrm{is}}^{\mathrm{decay}} + \gamma_{\mathrm{is}}^{\mathrm{drift}} + \kappa_{\mathrm{in}}$, where κ_{in} is the linewidth of the pumping laser. One has R [Hz] $\sim 10^{-5} \times \mathcal{E}^4$ [MV^4 m^{-4}] when Γ_{pump} is on a 10 kHz scale. When $\mathcal{E} = 1$ MV m^{-1}, one has $R \sim 10^{-5}$ Hz. If a [10 μm]^3 Na_2ThF_6 sample with a ^{229}Th number density of 10^{26} m^{-3} is

used, then there will be $\sim 10^6$ excitations to, and $\sim 10^2$ radiative decays from the isomeric state per second. This could be fast enough for the experimental observation of the nuclear radiative emission.

IV. POPULATION INVERSION UNDER TWO-STEP PUMPING

While the two-photon process discussed above can pump the isomeric state, it cannot lead to a population inversion, because it only involves two nuclear states. For population inversion, at least one other auxiliary state is necessary [33]. The second nuclear orbital excited state is not an ideal choice because its high energy (29 keV) necessitates demanding x-ray sources. A more practical option is to use the nuclear spin sublevels. However, the energy splitting between these spin sublevels is too small. Hence, if the common one-step pumping scheme is used, then an effective population can be achieved only under a cryogenic temperature of millikelvins (Sec. 3 in Ref. [28]).

For room-temperature nuclear lasing, we propose a two-step pumping process [Fig. 2(b)]. Initially, the system is at thermal equilibrium, so the ground-state sublevels have (approximately) the same population (normalized to $f = 1$), while the isomeric states are empty ($f = 0$). For the first step of the pumping process, we use a two-photon pumping laser resonant with the $|\mathrm{gr}, \pm 1/2\rangle \leftrightarrow |\mathrm{is}, \pm 1/2\rangle$ transition. Provided the pumping rate is large enough ($R \gg \gamma_{\mathrm{is}}^{\mathrm{decay}}$), the $|\mathrm{is}, \pm 1/2\rangle$ state will have almost the same population ($f = \frac{1}{2}$) as the $|\mathrm{gr}, \pm 1/2\rangle$ state when the pumping saturates. Then, we switch to a second pumping laser resonant with the $|\mathrm{gr}, \pm 1/2\rangle \leftrightarrow |\mathrm{is}, \pm 3/2\rangle$ transition, which again equalizes the final population ($f = \frac{1}{4}$) on these two states. This results in the population inversion between $|\mathrm{is}, \pm 1/2\rangle$ ($f = \frac{1}{2}$) and $|\mathrm{gr}, \pm 1/2\rangle$ ($f = \frac{1}{4}$), and nuclear lasing between these two states would start when the laser resonator is tuned on resonance. A greater population inversion can be achieved if a multistep pumping sequence is used (Sec. 3.2 in Ref. [28]). A caveat is that the two-photon pumping rate R should be faster than the nuclear spin relaxation, which tends to equalize the population among nuclear spin sublevels at room temperature and destroy the population inversion. Considering that the nuclear spin relaxation rate is usually on the order of Hz at room temperature [45,46], a pumping rate of $R = 100$ Hz should suffice. The corresponding pumping electric field is $\mathcal{E}_{\mathrm{in}} \approx 0.56$ MV/cm, and the laser power is $P_{\mathrm{in}} \approx 4.2$ W when the spot size is $[1\ \mu\mathrm{m}]^2$. With a pumping rate of $R = 100$ Hz, it takes 0.01–0.1 s to reach the two-level saturation. In addition, we remark that the linewidth of the pumping laser should be smaller than the splitting between nuclear spin sublevels (around 10 MHz in Na_2ThF_6), so that it can be resonant with just one nuclear transition at a time.

V. EXPERIMENTAL SETUP AND PERFORMANCE OF THE NUCLEAR LASER

Next, we discuss the basic experimental setup of the nuclear laser. We assume the gain medium (e.g., Na_2ThF_6) has a volume $V = Sl$, with S the cross-sectional area and l the length. The total number of *active* ^{229}Th nuclei is $N_{\mathrm{Th}} = f_n \rho_n V$, where ρ_n is the number density of ^{229}Th, while $f_n \approx 1$ is the Lamb-Mössbauer factor (also known as the Debye-Waller factor) [47]. For clarity, we fix $f_n \rho_n \sim 10^{26}$ m^{-3}, which can be achieved when ^{229}Th is enriched to $\sim 1\%$ abundance. Note that an abundance of ^{229}Th exceeding 75% has been realized before [48]. Given a gain medium with a 1 μm × 1 μm × 1 mm dimension (see below), the total weight of ^{229}Th nuclei is around 4×10^{-11} g, much smaller than the current global stock of ^{229}Th (tens of grams [1]). The total pumping rate is $\mathcal{R} \equiv N_{\mathrm{Th}} R \propto Sl\mathcal{E}^4$, while the total power of the pumping laser is $P_{\mathrm{in}} \propto S\mathcal{E}^2$, yielding $\mathcal{R} \propto \frac{P_{\mathrm{in}}^2 l}{S}$. Hence, a smaller S improves $\mathcal{R}$, as is typical for nonlinear two-photon processes [34]. Considering that the wavelength of the pumping laser is around 300 nm, we suggest using $S = [1\ \mu\mathrm{m}]^2$. On the other hand, the length l should not be too small, because the performance of the pulsed nuclear laser, including peak power and number of photons per pulse, increases with l. For demonstrative purposes, we will use $l = 1$ mm hereafter, but we have not optimized these parameters. The gain medium is thus a nanowire of size 1 μm × 1 μm × 1 mm. Actually, nanowire lasers have been demonstrated before based on electronic transitions [49].

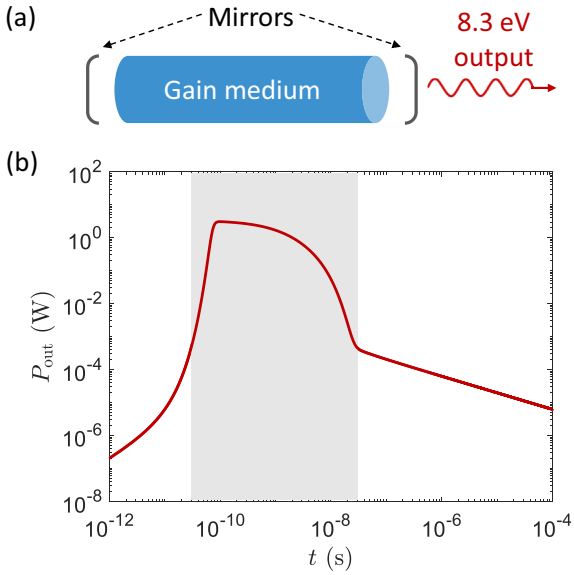

FIG. 3. (a) A simplified setup of the nuclear laser. (b) Time evolution of the output power of the nuclear laser. The parameters of the nuclear laser are described in the main text. The shaded area indicates a nuclear laser pulse.

We further assume that the nanowire gain medium is confined by two mirrors on two sides, which forms an optical cavity [Fig. 3(a)]. The left mirror is a total reflector with 100% reflectivity for the 8.3 eV cavity photon, while the right mirror is a partial reflector with a transmissivity of T, which serves as the output channel of the cavity photons. The stimulated emission (absorption) rate of the cavity photons can be expressed as $K = \frac{4|\langle \mathrm{gr}, m_{\mathrm{gr}}|\mathcal{M}_{M1}|\mathrm{is}, m_{\mathrm{is}}\rangle|^2 \mathcal{B}_{\mathrm{zpf}}^2}{\Gamma_0}$, where $\Gamma_0 \sim \gamma_{\mathrm{is}}^{\mathrm{decay}} + \gamma_{\mathrm{is}}^{\mathrm{drift}}$ is the total broadening of the isomeric states, $\mathcal{M}_{M1}$ is the nuclear magnetic dipole transition dipole, and $\mathcal{B}_{\mathrm{zpf}} = \sqrt{\frac{\mu_0 \omega_{\mathrm{is}}}{2V}}$ is the zero-point magnetic field of the cavity

photon with μ_0 the vacuum permittivity. Note that we only consider the $M1$ channel, as it is much more efficient than the $E2$ channel for radiative transitions that do not involve electrons [32].

The performance of the nuclear laser can be evaluated using the semiclassical rate equations (details in Sec. 4.1 in Ref. [28]). A typical time evolution of the output power P_{out} is plotted in Fig. 3(b), where one can clearly see a nuclear laser pulse with a peak power of above 1 W and a duration of about 10 ns [shaded area in Fig. 3(b)]. A total of 4.6×10^9 nuclear gamma photons (8.3 eV) will be emitted per pulse. Because these highly coherent and collinear photons come from the stimulated emission of the nuclear excited states, our device would qualify as a gamma-ray laser. In Sec. 4.2 of Ref. [28], we also show that the losses and temperature rise in the gain medium are minor and would not influence the operation of the nuclear laser.

Here we would like to remark on some potential challenges in constructing the nuclear laser proposed in this work. First, the nuclear lasing requires fast pumping of the nuclear isomeric state, so a ∼4.2 eV UV-B laser with narrow linewidth and high power, which are assumed to be 10 kHz and 1 W in the discussions above, would be necessary. Such a laser would be challenging to build, but we expect it could be easier than building an ∼8.3 eV FUV laser. Additionally, our proposal implicitly assumes that the isomeric transition energy ω_{is} is known with high precision, which has not been realized yet. Fortunately, ω_{is} has been measured with increasing precision [3] recently. Potentially, the two-photon ONQ pumping proposed in this work can be used to measure ω_{is}. To this purpose, one needs a pumping laser with tunable frequency, but the pumping rate does not necessarily need to be high, so a laser with relatively wide linewidth and low power may be sufficient.

In summary, we propose a two-photon pumping scheme to populate the long-lived nuclear isomer ^{229*}Th based on the ONQ effect in solid crystals. This pumping scheme could be used in nuclear clocks based on ^{229}Th as well. We further propose a nuclear gamma-ray laser (as this emission originates from nuclear isomeric transition) that utilizes ultrawide band gap ^{229}Th compounds as the gain medium and a two-step two-photon scheme to achieve population inversion at room temperature. Pulsed nuclear lasing should be realizable with a watt-level pumping laser. The nuclear laser with narrow linewidth might be useful for various applications in, e.g., nanoimaging, nuclear clock, and quantum information processing.

ACKNOWLEDGMENTS

We acknowledge support by DTRA (Award No. HDTRA1-20-2-0002), Interaction of Ionizing Radiation with Matter (IIRM), University Research Alliance (URA); and Office of Naval Research MURI through Grant No. N00014-17-1-2661.

[1] K. Beeks, T. Sikorsky, T. Schumm, J. Thielking, M. V. Okhapkin, and E. Peik, The thorium-229 low-energy isomer and the nuclear clock, Nat. Rev. Phys. **3**, 238 (2021).

[2] E. Peik, T. Schumm, M. S. Safronova, A. Pálffy, J. Weitenberg, and P. G. Thirolf, Nuclear clocks for testing fundamental physics, Quantum Sci. Technol. **6**, 034002 (2021).

[3] S. Kraemer *et al.*, Observation of the radiative decay of the ^{229}Th nuclear clock isomer, Nature **617**, 706 (2023).

[4] K. S. Krane, *Introductory Nuclear Physics*, 3rd ed. (Wiley, Hoboken, NJ, 1987).

[5] E. Ruchowska *et al.*, Nuclear structure of ^{229}Th, Phys. Rev. C **73**, 044326 (2006).

[6] N. Minkov and A. Pálffy, Reduced Transition Probabilities for the Gamma Decay of the 7.8 eV Isomer in ^{229}Th, Phys. Rev. Lett. **118**, 212501 (2017).

[7] S. G. Porsev, V. V. Flambaum, E. Peik, and C. Tamm, Excitation of the Isomeric ^{229m}Th Nuclear State via an Electronic Bridge Process in $^{229+}$ Th, Phys. Rev. Lett. **105**, 182501 (2010).

[8] E. V. Tkalya, Excitation of ^{229m}Th at Inelastic Scattering of Low Energy Electrons, Phys. Rev. Lett. **124**, 242501 (2020).

[9] B. S. Nickerson, M. Pimon, P. V. Bilous, J. Gugler, K. Beeks, T. Sikorsky, P. Mohn, T. Schumm, and A. Pálffy, Nuclear Excitation of the ^{229}Th Isomer via Defect States in Doped Crystals, Phys. Rev. Lett. **125**, 032501 (2020).

[10] E. Peik and C. Tamm, Nuclear laser spectroscopy of the 3.5 eV in Th-229, Europhys. Lett. **61**, 181 (2003).

[11] C. J. Campbell, A. G. Radnaev, A. Kuzmich, V. A. Dzuba, V. V. Flambaum, and A. Derevianko, Single-Ion Nuclear Clock for Metrology at the 19th Decimal Place, Phys. Rev. Lett. **108**, 120802 (2012).

[12] L. Von Der Wense *et al.*, Direct Detection of the ^{229}Th Nuclear Clock Transition, Nature (London) **533**, 47 (2016).

[13] V. V. Flambaum, Enhanced Effect of Temporal Variation of the Fine Structure Constant and the Strong Interaction in ^{229}Th, Phys. Rev. Lett. **97**, 092502 (2006).

[14] J. C. Berengut, V. A. Dzuba, V. V. Flambaum, and S. G. Porsev, Proposed Experimental Method to Determine α Sensitivity of Splitting between Ground and 7.6 eV Isomeric States in ^{229}Th, Phys. Rev. Lett. **102**, 210801 (2009).

[15] G. C. Baldwin and J. C. Solem, Recoilless gamma-ray lasers, Rev. Mod. Phys. **69**, 1085 (1997).

[16] L. A. Rivlin, Nuclear Gamma-Ray Laser: The Evolution of the Idea, Quantum Electron. **37**, 723 (2007).

[17] E. V. Tkalya, Proposal for a Nuclear Gamma-Ray Laser of Optical Range, Phys. Rev. Lett. **106**, 162501 (2011).

[18] T. Gouder, R. Eloirdi, R. L. Martin, M. Osipenko, M. Giovannini, and R. Caciuffo, Measurements of the band gap of ThF_4 by electron spectroscopy techniques, Phys. Rev. Res. **1**, 033005 (2019).

[19] P. V. Bilous, N. Minkov, and A. Pálffy, Electric quadrupole channel of the 7.8 EV ^{229}Th transition, Phys. Rev. C **97**, 044320 (2018).

[20] H. Xu, C. Li, G. Wang, H. Wang, H. Tang, A. R. Barr, P. Cappellaro, and J. Li, Two-Photon Interface of Nuclear Spins Based on the Optonuclear Quadrupolar Effect, Phys. Rev. X **13**, 011017 (2023).

[21] H. Xu, G. Wang, C. Li, H. Wang, H. Tang, A. R. Barr, P. Cappellaro, and J. Li, Laser Cooling of Nuclear Magnons, Phys. Rev. Lett. **130**, 063602 (2023).

[22] D. J. Elliott, *Ultraviolet Laser Technology and Applications* (Academic Press, New York, 1995).

[23] V. A. Krutov and V. N. Fomenko, Influence of electronic shell on gamma radiation of atomic nuclei, Ann. Phys. **476**, 291 (1968).

[24] M. Morita, Nuclear excitation by electron transition and its application to uranium 235 separation, Prog. Theor. Phys. **49**, 1574 (1973).

[25] R. A. Müller, A. V. Volotka, and A. Surzhykov, Excitation of the ^{229}Th nucleus via a two-photon electronic transition, Phys. Rev. A **99**, 042517 (2019).

[26] N. Q. Cai, G. Q. Zhang, C. B. Fu, and Y. G. Ma, Populating ^{229m}Th via two-photon electronic bridge mechanism, Nucl. Sci. Tech. **32**, 1 (2021).

[27] J. Yan *et al.*, Precision control of gamma-ray polarization using a crossed helical undulator free-electron laser, Nat. Photonics **13**, 629 (2019).

[28] See Supplemental Material at http://link.aps.org/supplemental/10.1103/PhysRevA.108.L021502 for detailed discussions on the properties of the Th compounds and the performance of the nuclear lasers.

[29] J. P. Perdew, K. Burke, and M. Ernzerhof, Generalized Gradient Approximation Made Simple, Phys. Rev. Lett. **77**, 3865 (1996).

[30] P. E. Blöchl, Projector augmented-wave method, Phys. Rev. B **50**, 17953 (1994).

[31] H. Tang, A. R. Barr, G. Wang, P. Cappellaro, and J. Li, First-principles calculation of the temperature-dependent transition energies in spin defects, J. Phys. Chem. Lett. **14**, 3266 (2023).

[32] E. V. Tkalya, C. Schneider, J. Jeet, and E. R. Hudson, Radiative lifetime and energy of the low-energy isomeric level in ^{229}Th, Phys. Rev. C **92**, 054324 (2015).

[33] O. Svelto, *Principles of Lasers* (Springer, New York, 2010).

[34] Y.-R. Shen, *The Principles of Nonlinear Optics* (Wiley, Hoboken, NJ, 1984).

[35] M. M. Choy and R. L. Byer, Accurate second-order susceptibility measurements of visible and infrared nonlinear crystals, Phys. Rev. B **14**, 1693 (1976).

[36] J. M. Hales, S.-H. Chi, T. Allen, S. Benis, N. Munera, J. W. Perry, D. McMorrow, D. J. Hagan, and E. W. Van Stryland, Third-order nonlinear optical coefficients of Si and GaAs in the near-infrared spectral region, in 2018 Conference on Lasers and Electro-Optics (CLEO) (IEEE, New York, 2018).

[37] G. Kresse and J. Furthmüller, Efficiency of *ab-initio* total energy calculations for metals and semiconductors using a plane-wave basis set, Comput. Mater. Sci. **6**, 15 (1996).

[38] G. Kresse and J. Furthmüller, Efficient iterative schemes for *ab initio* total-energy calculations using a plane-wave basis set, Phys. Rev. B **54**, 11169 (1996).

[39] E. V. Tkalya and R. Si, Internal conversion of the low-energy ^{229m}Th isomer in the thorium anion, Phys. Rev. C **101**, 054602 (2020).

[40] E. V. Tkalya, Spontaneous emission probability for M1 transition in a dielectric medium: ^{229m}Th ($3/2+$, 3.5 ± 1.0 eV) decay, JETP Lett. **71**, 311 (2000).

[41] C. J. Campbell, A. G. Radnaev, and A. Kuzmich, Wigner Crystals of ^{229}Th for Optical Excitation of the Nuclear Isomer, Phys. Rev. Lett. **106**, 223001 (2011).

[42] P. Dessovic, P. Mohn, R. A. Jackson, G. Winkler, M. Schreitl, G. Kazakov, and T. Schumm, ^{229}Th orium-doped calcium fluoride for nuclear laser spectroscopy, J. Phys.: Condens. Matter **26**, 105402 (2014).

[43] W. G. Rellergert, D. Demille, R. R. Greco, M. P. Hehlen, J. R. Torgerson, and E. R. Hudson, Constraining the Evolution of the Fundamental Constants with a Solid-State Optical Frequency Reference Based on the ^{229}Th Nucleus, Phys. Rev. Lett. **104**, 200802 (2010).

[44] J. D. Jackson, *Classical Electrodynamics*, 3rd ed. (Wiley, Hoboken, NJ, 1999).

[45] P. J. Hore, *Nuclear Magnetic Resonance* (Oxford University Press, Oxford, 2015).

[46] R. V. Pound, Nuclear spin relaxation times in single crystals of LiF, Phys. Rev. **81**, 156 (1951).

[47] N. N. Greenwood and T. C. Gibb, *Mössbauer Spectroscopy* (Springer, Berlin, 1971).

[48] J. Jeet, C. Schneider, S. T. Sullivan, W. G. Rellergert, S. Mirzadeh, A. Cassanho, H. P. Jenssen, E. V. Tkalya, and E. R. Hudson, Results of a Direct Search Using Synchrotron Radiation for the Low-Energy ^{229}Th Nuclear Isomeric Transition, Phys. Rev. Lett. **114**, 253001 (2015).

[49] M. H. Huang, S. Mao, H. Feick, H. Yan, Y. Wu, H. Kind, E. Weber, R. Russo, and P. Yang, Room-temperature ultraviolet nanowire nanolasers, Science **292**, 1897 (2001).

Erratum: Solid-state ^{229}Th nuclear laser with two-photon pumping [Phys. Rev. A 108, L021502 (2023)]

Haowei Xu, Hao Tang, Guoqing Wang, Changhao Li, Boning Li, Paola Cappellaro, and Ju Li

(Received 7 September 2025; published 29 September 2025)

DOI: 10.1103/vmb6-z954

In Sec. V of our original article, the stimulated emission (absorption) rate of the cavity photons was defined as $K = \frac{4|\langle \mathrm{gr}, m_{\mathrm{gr}}|\mathcal{M}_{M1}|\mathrm{is}, m_{\mathrm{is}}\rangle|^2 \mathcal{B}_{\mathrm{zpf}}^2}{\Gamma_0}$ and the denominator Γ_0 was incorrectly taken as $\gamma_{\mathrm{is}}^{\mathrm{decay}} + \gamma_{\mathrm{is}}^{\mathrm{drift}}$. The correct denominator should be $\Gamma_0 = \gamma_{\mathrm{is}}^{\mathrm{decay}} + \gamma_{\mathrm{is}}^{\mathrm{drift}} + \beta$, where $\beta = \frac{c_0(1-R)}{2l}$ is the cavity photon decay rate due to the output channel. Here c_0 is the speed of light, l is the length of the gain medium, and R is the transmittance of the right mirror [Fig. 3(a)]. Using this corrected formula, discussion relevant to the performance of the nuclear laser [i.e., Fig. 3(b)] should be revised. Here we propose two schemes for the operation of the nuclear laser.

(i) Fixed mirror reflectivity. We use the same parameters as in the paper, except for a new $R = 99.99\%$. The stimulated emission rate K becomes much smaller due to the large β. As a result, the peak power of the nuclear laser would drop to the nanowatt range, but the pulse would last for about 1 s [revised Fig. 1(a)]. The total number of γ-ray photons emitted per pulse remains on the order of 10^9. In short, this yields a weaker but longer pulse, compared to Fig. 3(b) in the original article.

(ii) Switched mirror reflectivity. One can use, for example, a chopper wheel or electrically tunable mirror to switch the reflectivity of the mirror. The mirror reflectivity is kept at a high value R_1 for some duration t_1, leading to a relatively large K and efficient stimulated emission of γ-ray photons, which accumulate in the cavity. For a subsequent duration t_2, the reflectivity is reduced to a small value R_2, allowing photons to quickly couple out, generating a strong and short γ-ray pulse. Periodic switching could produce a train of such strong and short pulses. Using $R_1 = 99.99\%$, $t_1 = 10^{-4}$ s, $R_2 = 10\%$, and $t_2 = 10^{-6}$ s, the simulated pulse train is shown in the revised Fig. 1(b).

We thank Karen Mamian and Charles Roques-Carmes for pointing out this mistake.

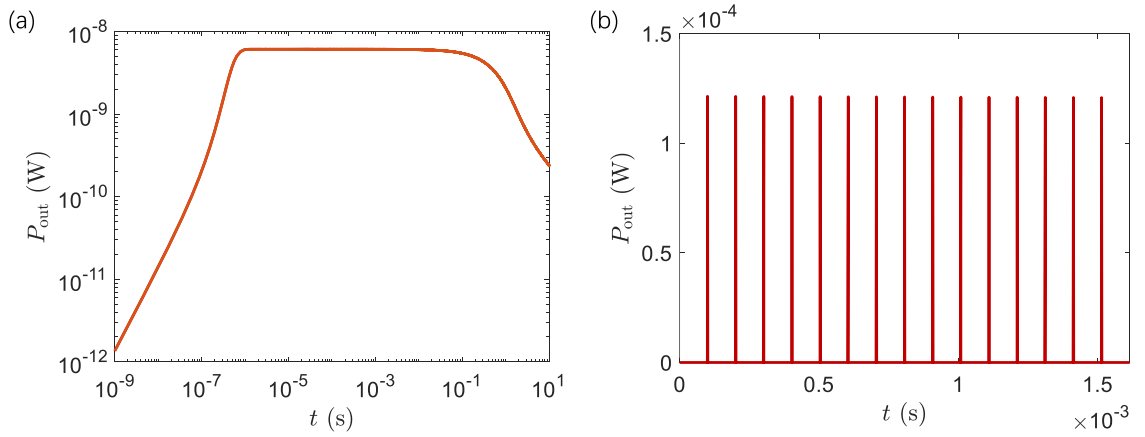

FIG. 1. Two schemes for the operation of the nuclear laser: (a) fixed mirror reflectivity, yielding a single weak but long pulse, and (b) switched mirror reflectivity, yielding a series of strong but short pulses.

